nature portfolio

https://doi.org/10.1038/s41586-024-07817-y

Supplementary information

Molecular architecture of coronavirus double-membrane vesicle pore complex

In the format provided by the authors and unedited

Supplementary information

Molecular Architecture of Coronavirus Double Membrane Vesicle Pore Complex

Yixin Huang[1], Tongyun Wang[2], Lijie Zhong[1], Wenxin Zhang[1], Yu Zhang[1], Xiulian Yu[3], Shuofeng Yuan[2,#] & Tao Ni[1,4,#]

[1]School of Biomedical Sciences, Li Ka Shing Faculty of Medicine, The University of Hong Kong, Pokfulam, Hong Kong SAR, China.

[2]State Key Laboratory of Emerging Infectious Diseases, Carol Yu Centre for Infection, Department of Microbiology, Li Ka Shing Faculty of Medicine, The University of Hong Kong, Pokfulam, Hong Kong SAR, China.

[3]Department of Applied Biology and Chemical Technology, Faculty of Science, The Hong Kong Polytechnic University, Hung Hom, Kowloon, Hong Kong SAR, China.

[4]Materials Innovation Institute for Life Sciences and Energy (MILES), HKU-SIRI, Shenzhen, P.R. China

corresponding authors: Tao Ni, Email: taoni@hku.hk; Shuofeng Yuan, Email: yuansf@hku.hk

Table of Contents

Supplementary Figures

Supplementary Fig. 1 Purification results of double membrane vesicles containing. nsp3 and nsp4.

Supplementary Fig. 2 Alphafold prediction of nsp3 (417-1945).

Supplementary Fig. 3 Alphafold prediction of nsp4.

Supplementary Fig. 4 Alphafold prediction of nsp3-4 ectodomain complex.

Supplementary Fig. 5 Alphafold prediction of Mac2-3_NAB complex.

Supplementary Fig. 6 Local quality of model fitting to cryo-ET density maps by Q-scores.

Supplementary Fig. 7 Assessment of model overfitting by LDDT scores.

Supplementary Fig. 8 Flow cytometric analysis of VeroE6 cells.

Supplementary Fig. 9 Co-IP of nsp3 and nsp4 pore complex mutants.

Supplementary Figures

Supplementary Fig. 1 Purification results of double membrane vesicles containing nsp3 and nsp4.

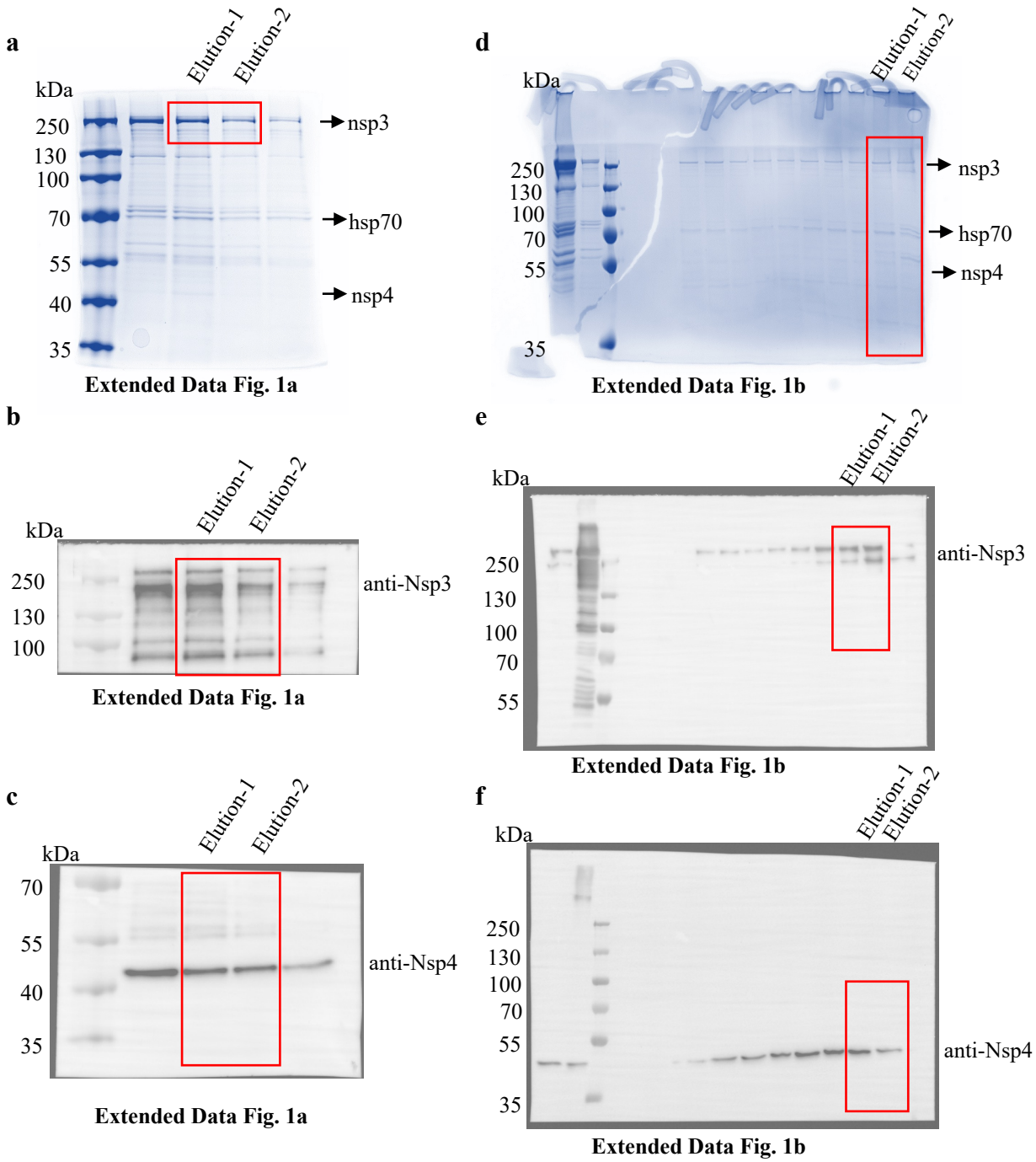

Supplementary Fig. 1 | Purification results of double membrane vesicles containing nsp3 and nsp4. (**a-c**) SDS-PAGE analysis and Western blot of none-detergent-treated DMV sample for **Extended Data Fig. 1a**. SDS-PAGE gel shows elution fraction after StrepTactin affinity purification (**a**), western blot results with anti-nsp3 and anti-nsp4 antibodies are shown in (**b**) and (**c**), respectively. (**d-f**) SDS-PAGE analysis and western blot of detergent-extracted nsp3-4 complex for **Extended Data Fig. 1b**. SDS-PAGE gel shows elution fraction after StrepTactin affinity purification (**d**), western blot results with anti-nsp3 and anti-nsp4 antibodies are shown in (**e**) and (**f**), respectively. The red rectangles show the cropping location.

Supplementary Fig. 2 Alphafold prediction of nsp3 (417-1945).

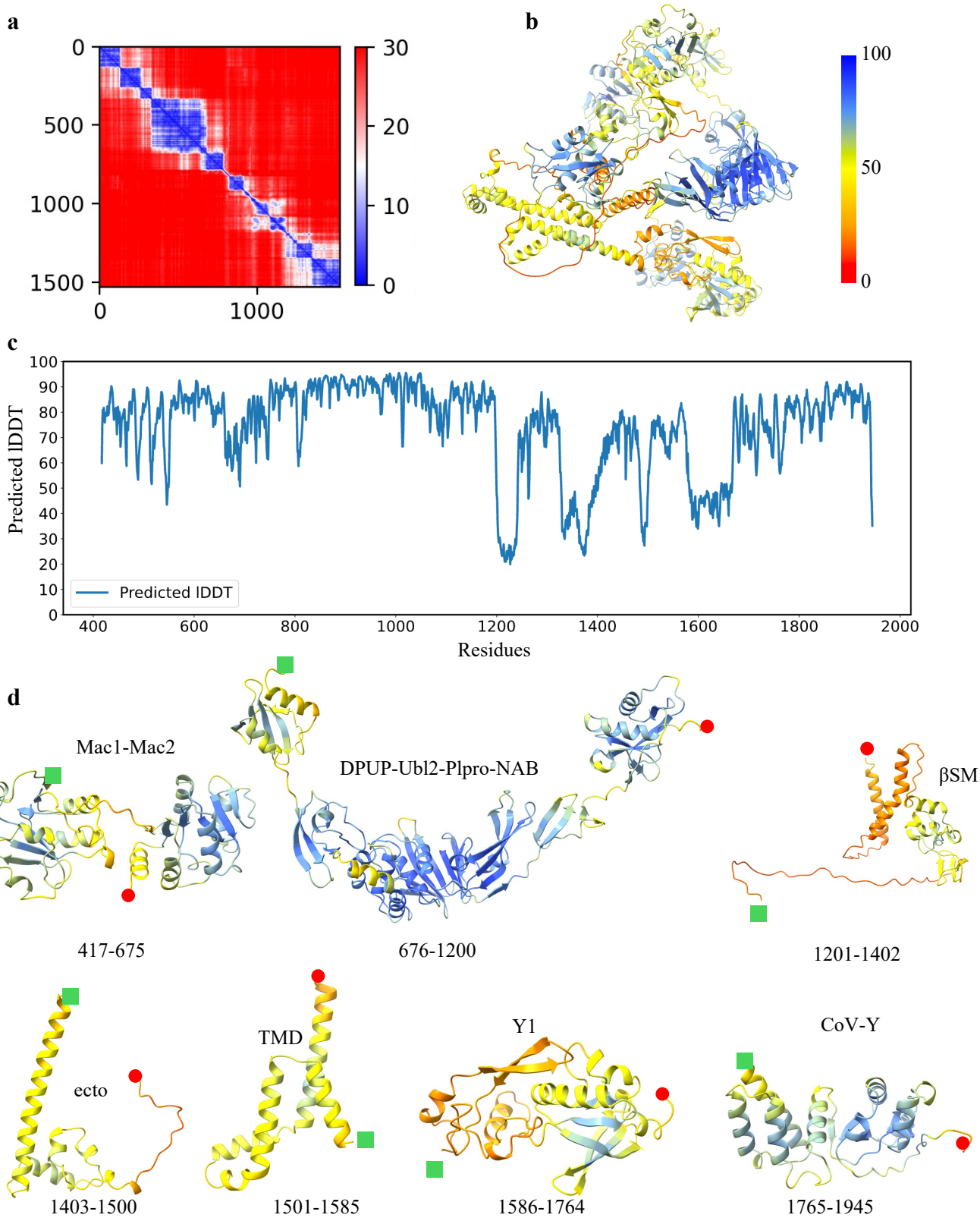

Supplementary Fig. 2 | Alphafold prediction of nsp3 (417-1945). (**a**) Predicted Aligned Error (PAE) plot, showing regions of high confidence (dark blue) and low confidence (red). (**b**) Predicted structure of nsp3(417-1945) colored by pLDDT from 0 to 100 (red to blue). (**c**) Per-residue plot of pLDDT (predicted local distance difference test) scores. (**d**) Domain structures of nsp3(417-1945) colored by pLDDT. The green square and red dot represent the N-terminus and C-terminus of domains, respectively.

Supplementary Fig. 3 Alphafold prediction of nsp4.

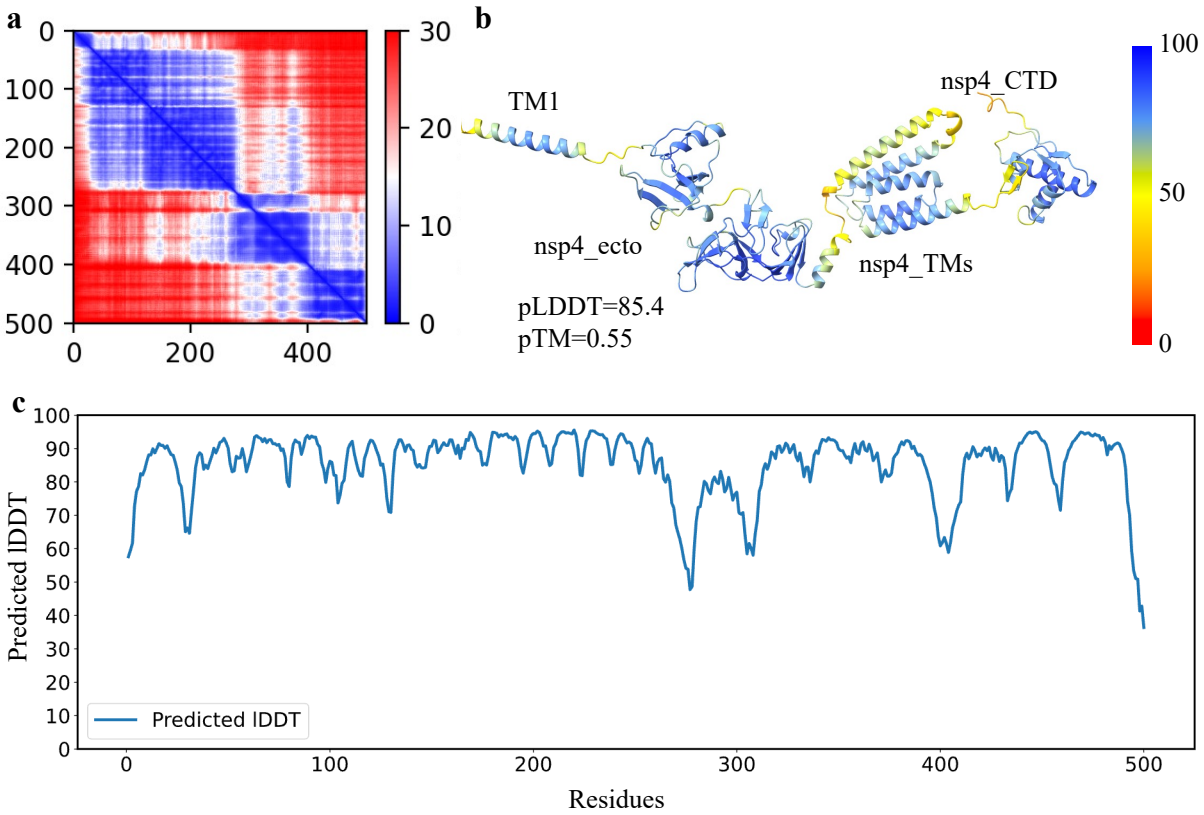

Supplementary Fig. 3 | Alphafold prediction of nsp4. (**a**) Predicted Aligned Error (PAE) plot, showing regions of high confidence (dark blue) and low confidence (red). (**b**) Predicted structure of nsp4 colored by pLDDT from 0 to 100 (red to blue). (**c**) Per-residue plot of pLDDT.

Supplementary Fig. 4 Alphafold prediction of nsp3-4 ectodomain complex.

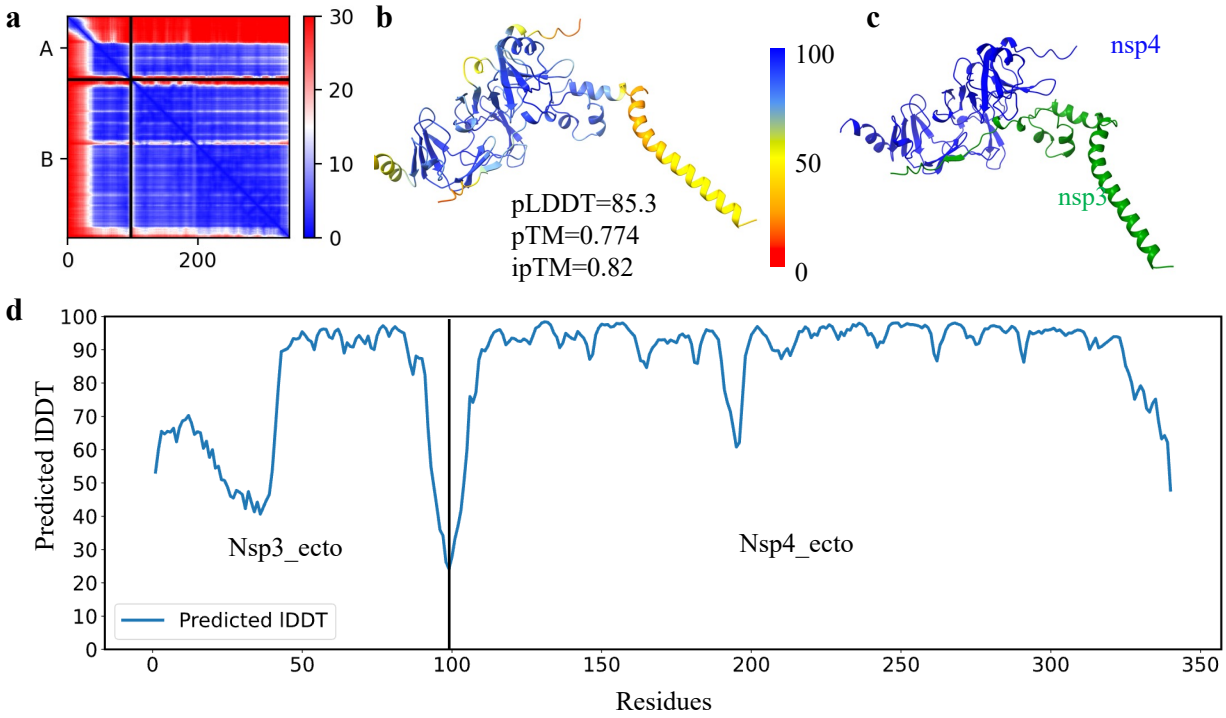

Supplementary Fig. 4 | Alphafold prediction of nsp3-4 ectodomain complex. (**a**) Predicted Aligned Error (PAE) plot, showing regions of high confidence (dark blue) and low confidence (red). (**b**) Predicted structure of nsp3-4 ectodomain complex colored by pLDDT from 0 to 100 (red to blue). (**c**) Predicted structure of nsp3-4 ectodomain complex colored by protein chains. (d) Per-residue plot of pLDDT.

Supplementary Fig. 5 Alphafold prediction of Mac2-3_NAB complex.

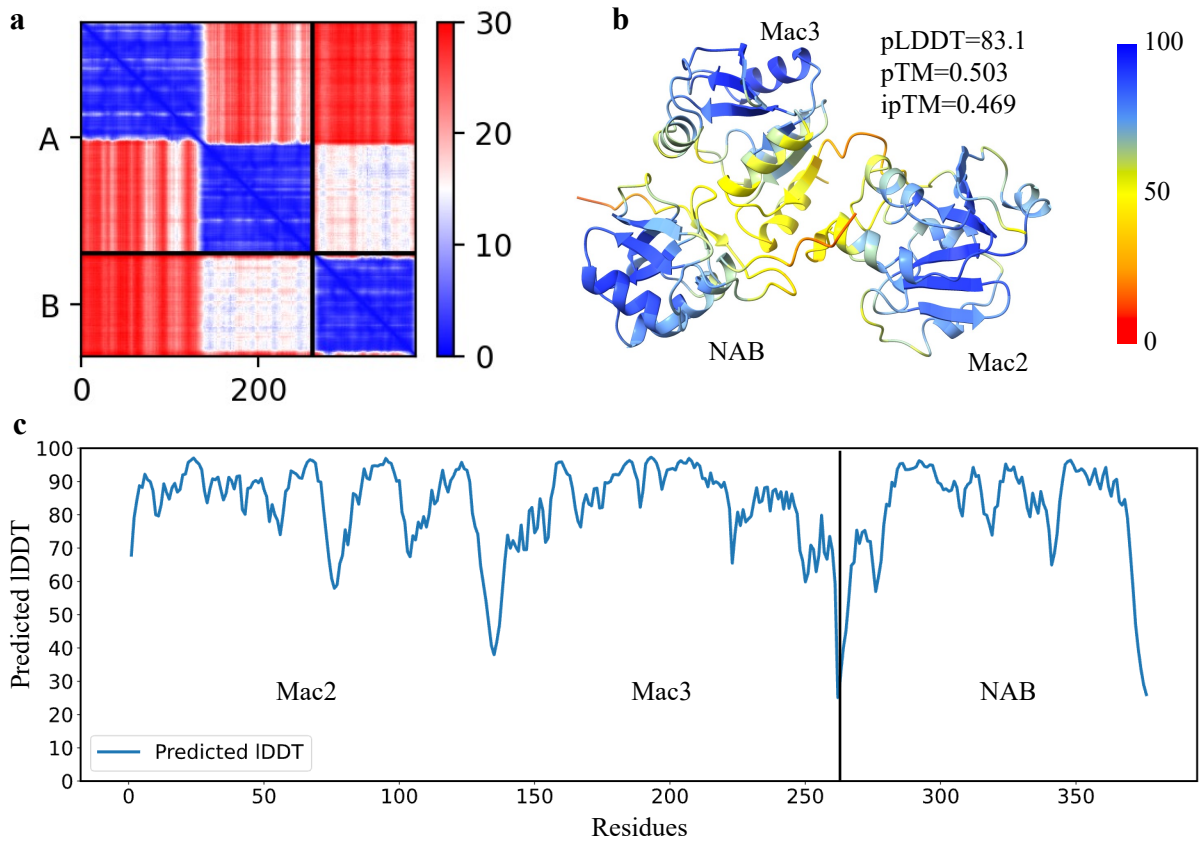

Supplementary Fig. 5 | Alphafold prediction of Mac2-3_NAB complex. (**a**) Predicted Aligned Error (PAE) plot, showing regions of high confidence (dark blue) and low confidence (red). (**b**) Predicted structure of Mac2-3_NAB complex colored by pLDDT from 0 to 100 (red to blue). (**c**) Per-residue plot of pLDDT.

Supplementary Fig. 6 Local quality of model fitting to cryo-ET density maps by Q-scores.

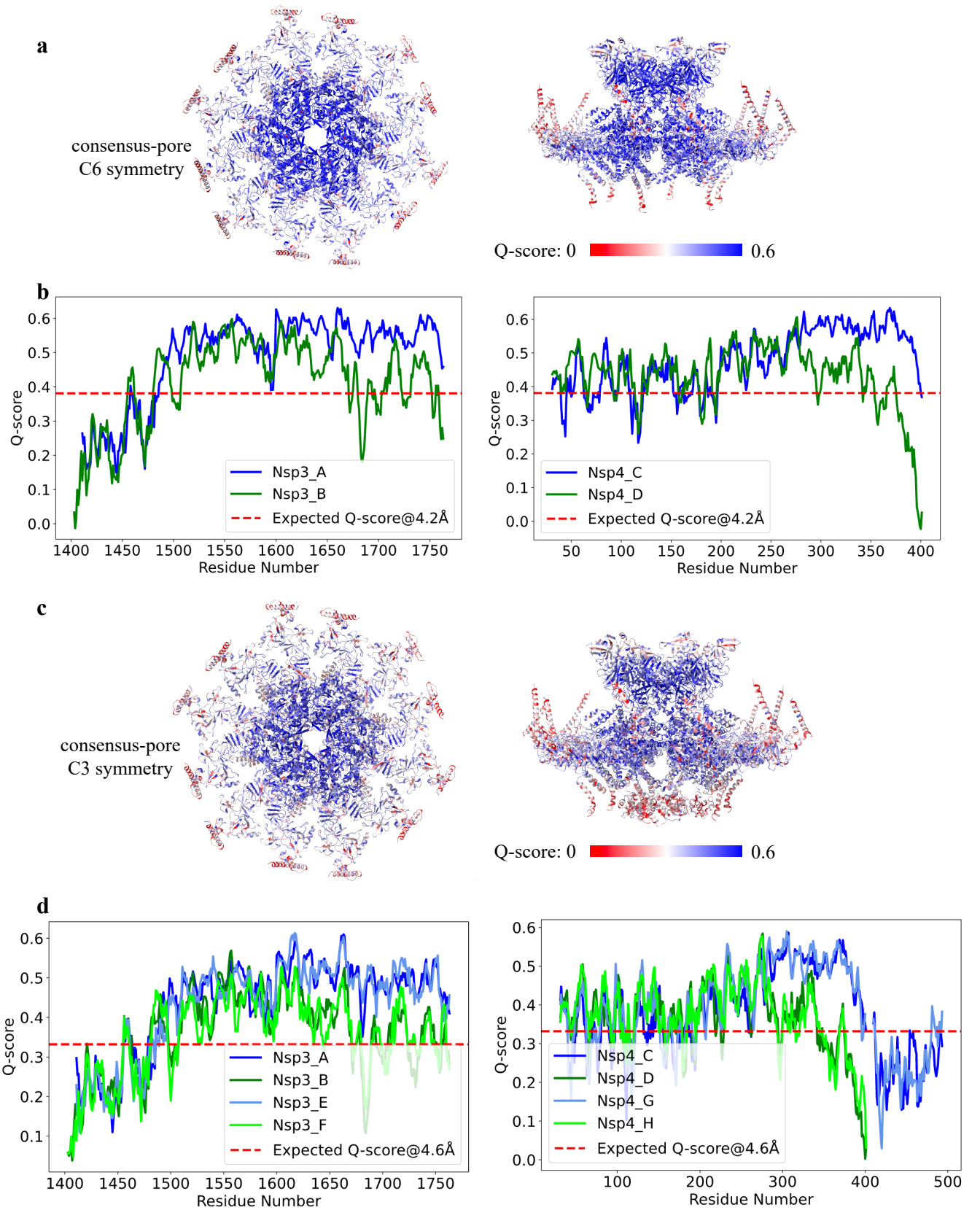

See figure legends next page

Supplementary Fig. 6 Local quality of model fitting to cryo-ET density maps by Q-scores.

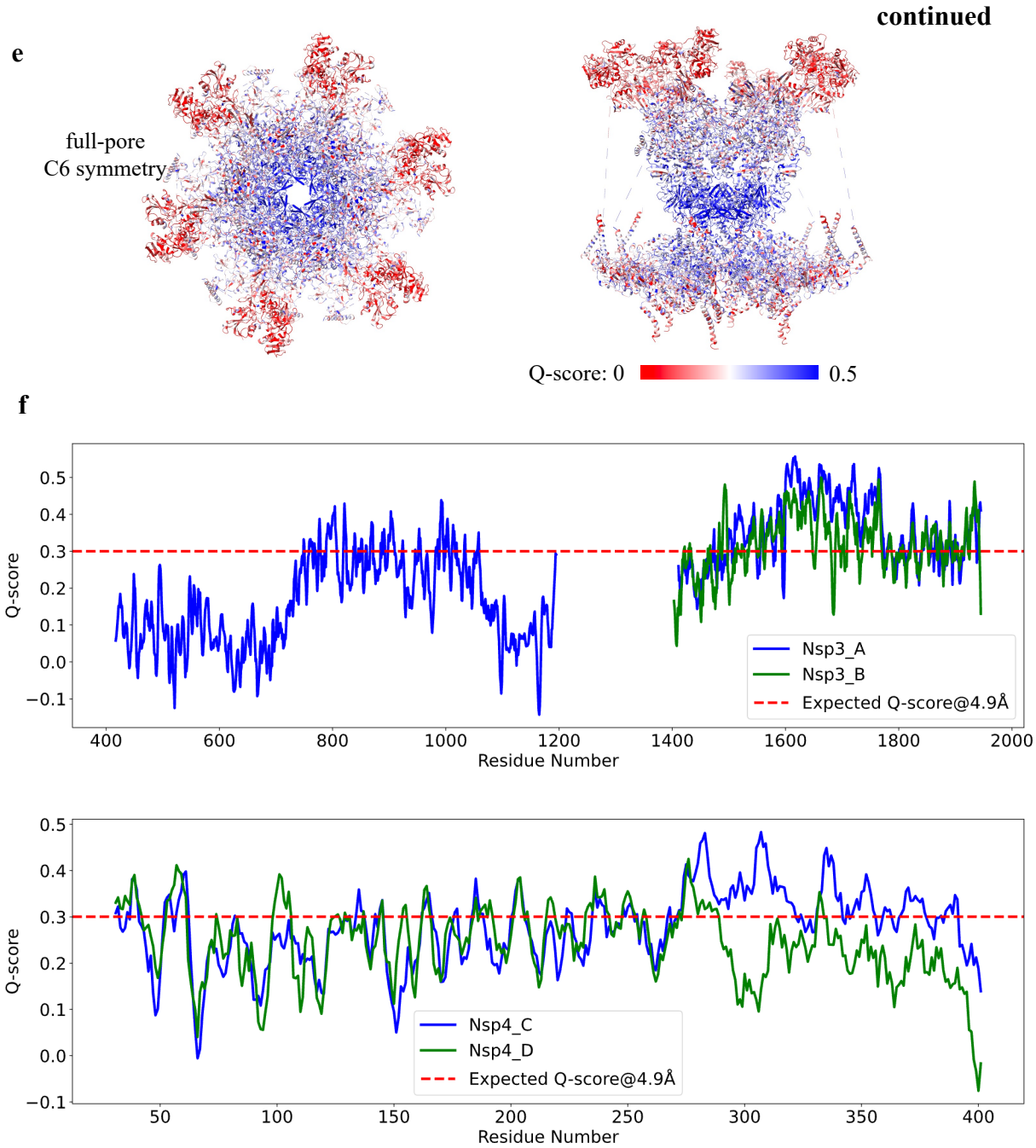

Supplementary Fig. 6 | Local quality of model fitting to cryo-ET density maps by Q-scores. (**a**) Structure of the C6 symmetrized consensus-pore in two orthogonal views, colored by per-residue Q-scores from red to blue (low Q-score to high Q-score). (**b**) Q-score plot of nsp3 and nsp4 chains in the asymmetric unit. The expected Q-score at 4.2 Å resolution is shown as dashed lines. The 5-residue average of Q-scores is plotted here. (**c-d**) Structure of C3 symmetrized consensus-pore colored by per-residue Q-scores and the corresponding Q-score plot. (**e-f**) Structure of the C6 symmetrized full-pore colored by per-residue Q-scores and the corresponding Q-score plot.

Supplementary Fig. 7 Assessment of model overfitting by LDDT scores.

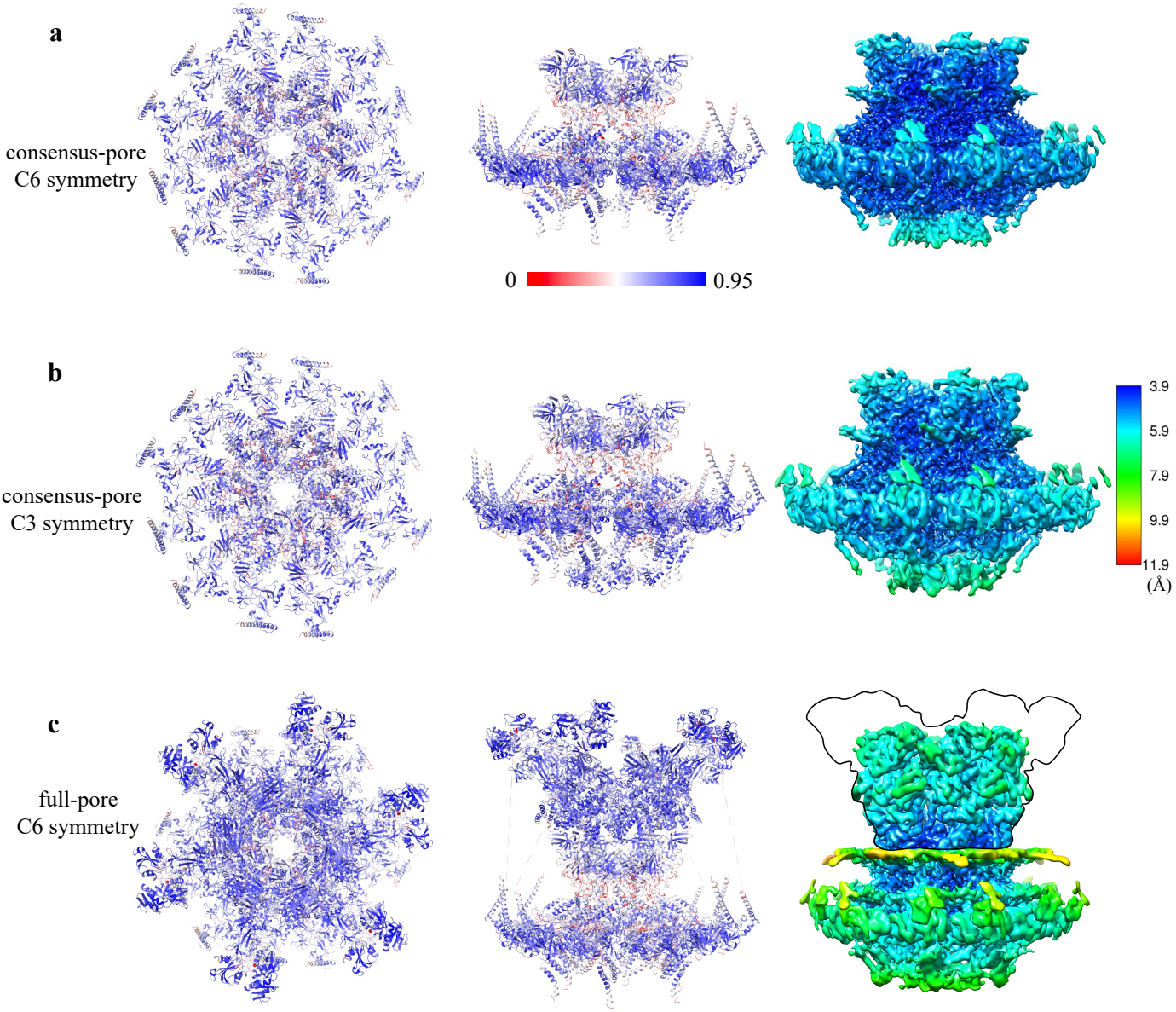

Supplementary Fig. 7 | Assessment of model overfitting by LDDT scores. Two orthogonal views of the six-fold symmetrized consensus-pore (**a**), three-fold symmetrized consensus-pore (**b**) and C6 symmetrized full-pore colored by LDDT (**c**), compared with their corresponding local-resolution estimation maps. The LDDT score was calculated by comparing the refined model with their Alphafold predicted models in Supplementary Fig. 2 and 3 using the online server (https://swissmodel.expasy.org/assess). The models are presented with the calculated LDDT scores colored from red to blue (0-0.95). The low LDDT regions do not match with the local resolution regions, indicating minimal overfitting issues.

Supplementary Fig. 8 Flow cytometric analysis of VeroE6 cells.

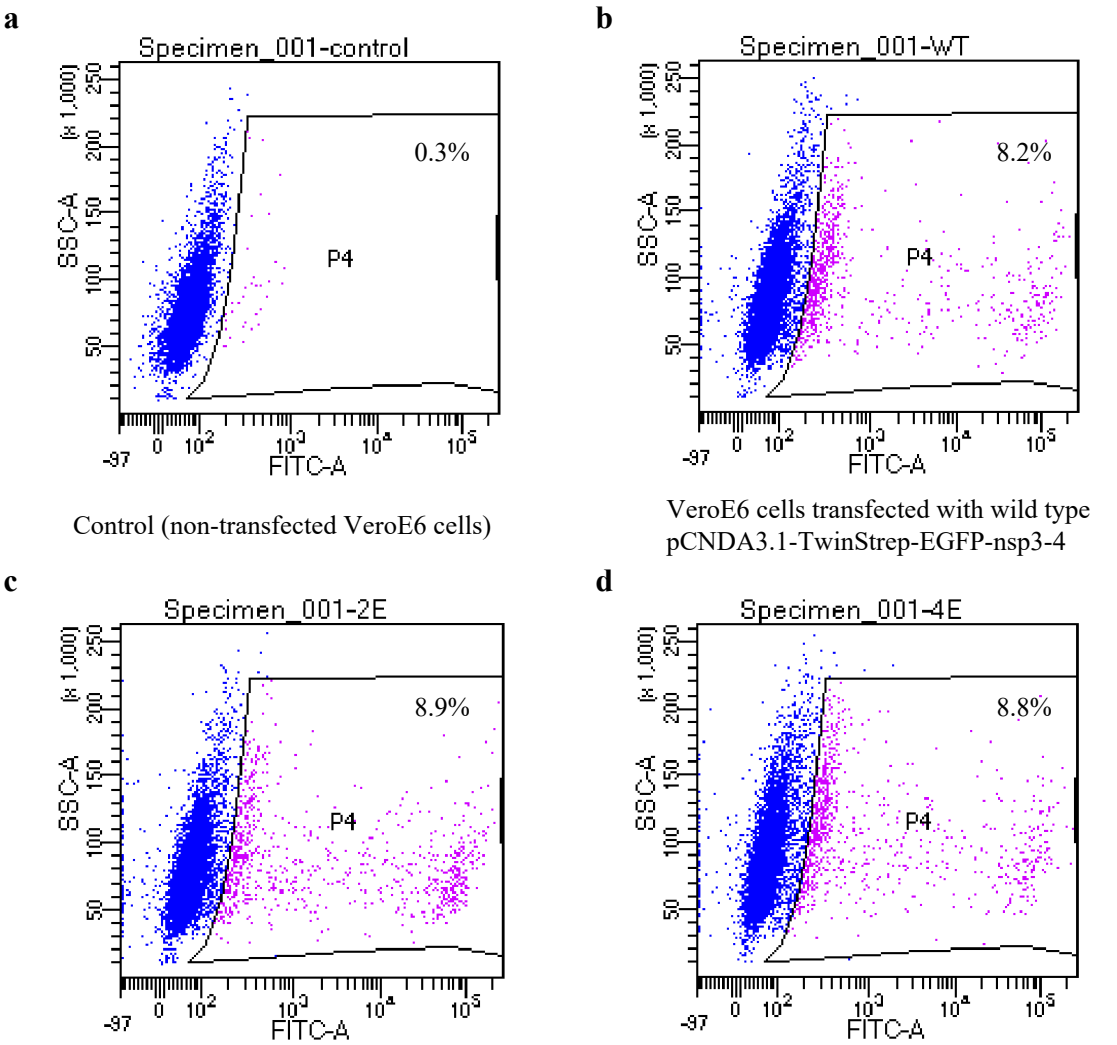

Control (non-transfected VeroE6 cells)

VeroE6 cells transfected with wild type pCNDA3.1-TwinStrep-EGFP-nsp3-4

VeroE6 cells transfected with mutant pCDNA3.1-TwinStrep-EGFP-nsp3-4 (nsp3 V1458E, L1480E)

VeroE6 cells transfected with mutant pCDNA3.1-TwinStrep-EGFP-nsp3-4 (nsp3 D1478E, Y1483E, L1486E, Q1490E)

Supplementary Fig. 8 | Flow cytometric analysis of VeroE6 cells. FACS plots (SSC-A) showing VeroE6 cells transfected with control **(a)**, wild type **(b)** or mutants **(c, d)**. In FACS plots, the percentage of sorted cells within total cells indicated in P4 area. FACS analysis was performed with a 488 nm laser. Cells were considered positive when the fluorescence intensity was above a threshold value which was determined by the maximum intensity of the non-transfected control cells.

Supplementary Fig. 9 Co-IP of nsp3 and nsp4 pore complex mutants.

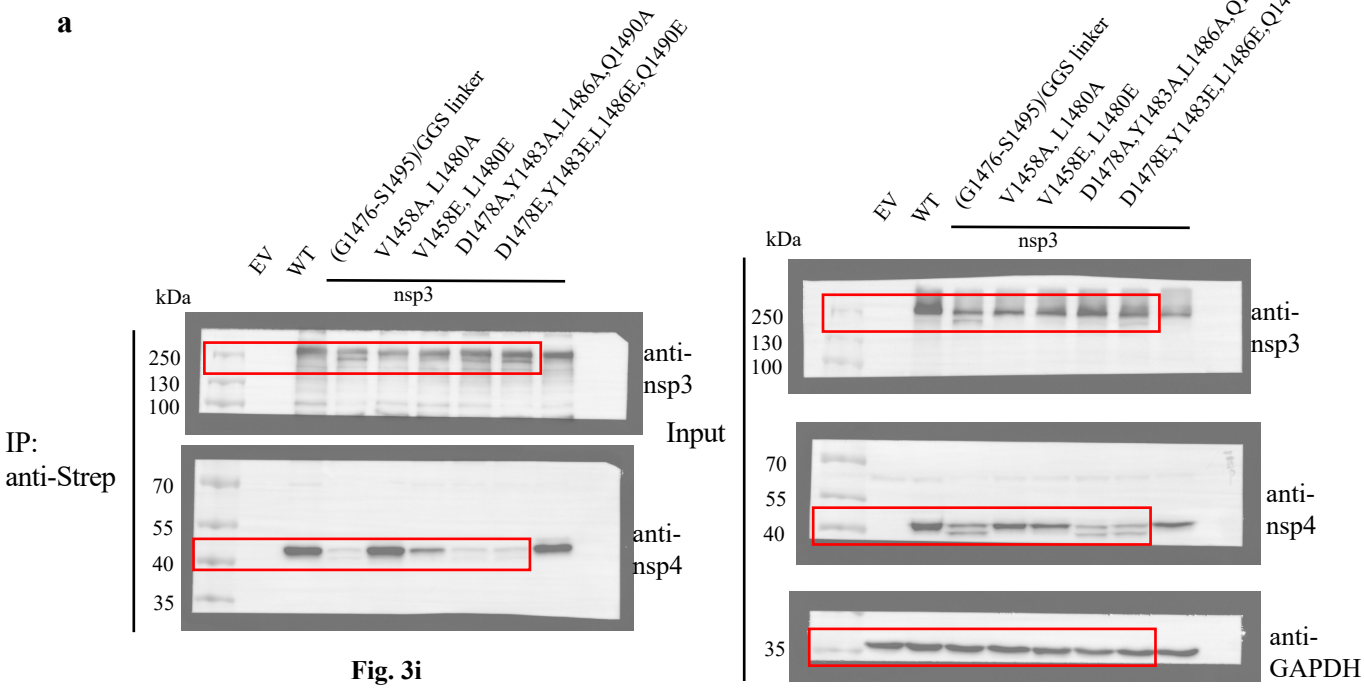

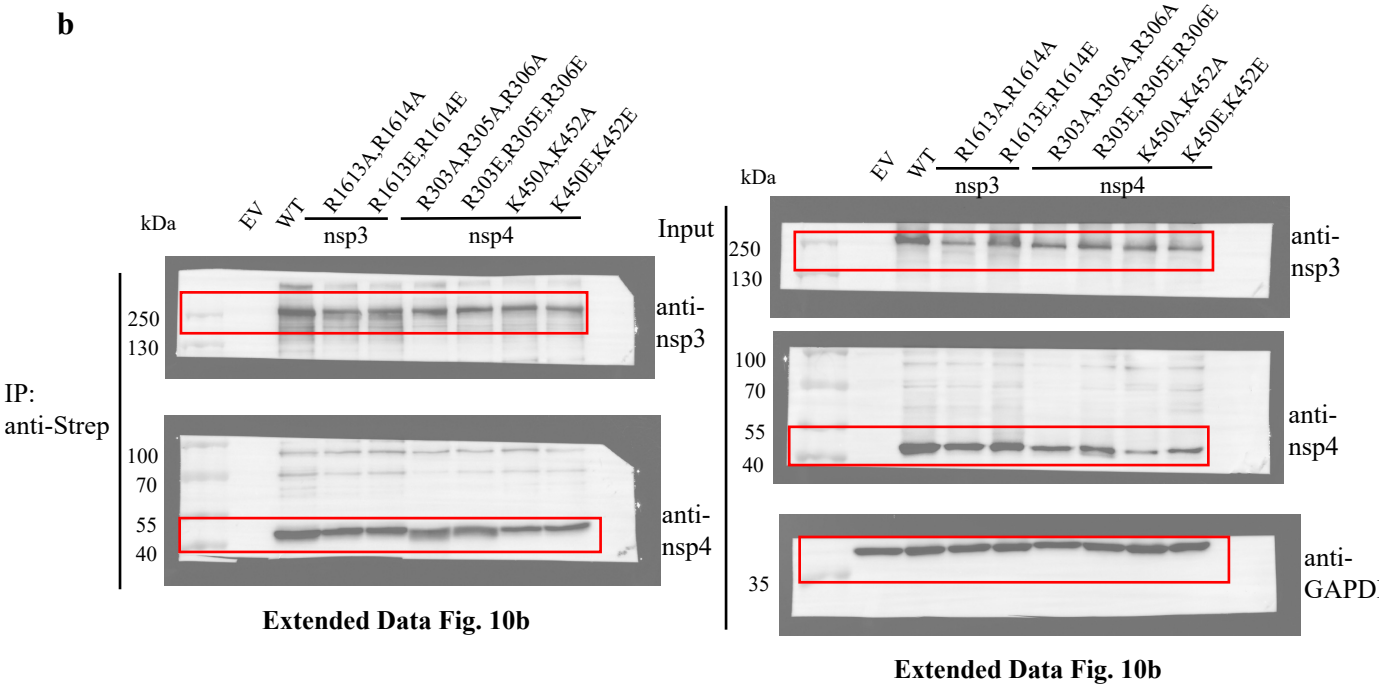

Supplementary Fig. 9 | Co-IP of nsp3 and nsp4 pore complex mutants. (**a**) Co-immunoprecipitation assay of mutants on nsp3-4 interfaces showing the interaction between nsp3 and nsp4 for **Fig. 3i**. TwinStrep-EGFP-nsp3 were co-IP with the StrepTactin beads. Nsp3, nsp4 and GAPDH were detected using anti-nsp3, anti-nsp4 and anti-GAPDH antibodies, respectively. For co-IP product, the blot from the same gel was probed with anti-nsp3 and nsp-4 antibodies. For the input product, nsp3 and GAPDH loading control were probed on the sample gel using anti-nsp3 and anti-GAPDH antibodies. The same sample was probed with antibody against nsp4 on a separate gel. (**b**) Co-immunoprecipitation assay of nsp3 and nsp4 pore mutants showing the interaction between nsp3 and nsp4 for **Extended Data Fig. 10b**. TwinStrep-EGFP-nsp3 were co-IP with the StrepTactin beads. Nsp3, nsp4 and GAPDH were detected using anti-nsp3, anti-nsp4 and anti-GAPDH antibodies, respectively. For co-IP or input product, the same blot was cut into two or three subregions to be probed with the corresponding antibodies. The red rectangles show the cropped area for data shown in **Extended Data Fig. 10b**.